

# LOBG: Less Overfitting for Better Generalization in Vision-Language Model

Chenhao Ding<sup>1</sup> Xinyuan Gao<sup>1</sup> Songlin Dong<sup>2</sup> Yuhange He<sup>2</sup>  
 Qiang Wang<sup>1</sup> Alex Kot<sup>3</sup> Yihong Gong<sup>1, 2</sup>

<sup>1</sup>School of Software Engineering, Xi'an Jiaotong University

<sup>2</sup>College of Artificial Intelligence, Xi'an Jiaotong University

<sup>3</sup>Nanyang Technological University

## Abstract

Existing prompt learning methods in Vision-Language Models (VLM) have effectively enhanced the transfer capability of VLM to downstream tasks, but they suffer from a significant decline in generalization due to severe overfitting. To address this issue, we propose a framework named **LOBG** for vision-language models. Specifically, we use CLIP to filter out fine-grained foreground information that might cause overfitting, thereby guiding prompts with basic visual concepts. To further mitigate overfitting, we developed a structural topology preservation (STP) loss at the feature level, which endows the feature space with overall plasticity, allowing effective reshaping of the feature space during optimization. Additionally, we employed hierarchical logit distillation (HLD) at the output level to constrain outputs, complementing STP at the output end. Extensive experimental results demonstrate that our method significantly improves generalization capability and alleviates overfitting compared to state-of-the-art approaches.

## 1. Introduction

Vision-language models (VLMs), such as CLIP [27] and ALIGN [12], have shown exceptional generalization capabilities for downstream tasks [6, 17, 20]. Prompt learning has emerged as a more efficient alternative to fine-tuning VLMs, such as CoOp [44], introducing learnable prompt vectors to adapt models for downstream tasks. However, since prompts are optimized for specific tasks, prompt models tend to overfit as training progresses, losing the original CLIP model’s ability to generalize to unseen tasks. Thus, maintaining generalization to unseen tasks while learning specific tasks is a crucial challenge in prompt learning, known as **Base to Novel** (B2N) [43] prompt learning.

The present mainstream approaches for the B2N task can be divided into categories: (i) Learning class-agnostic or independent prompts to reduce prompt overfitting [14, 43].

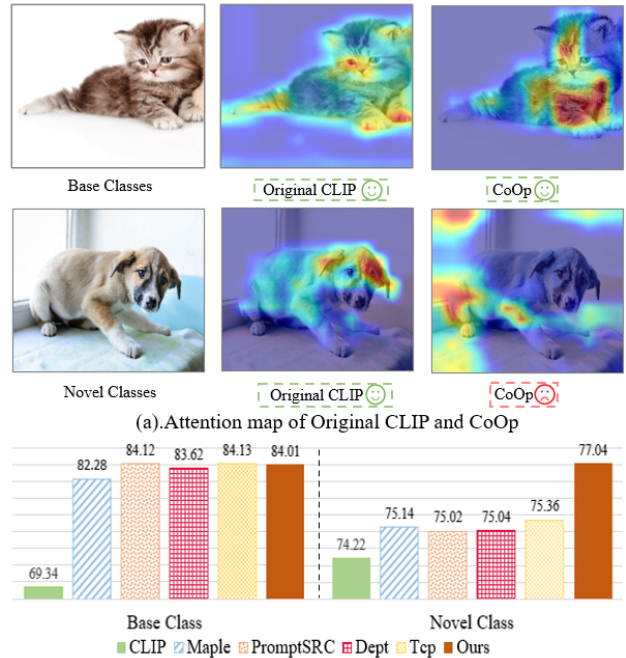


Figure 1. (a) Attention maps of CLIP and CoOp. Overfitting leads to more attention on fine details of base classes (e.g., a cat’s face). The overfitted model (e.g., CoOp) struggles to transfer learned knowledge to unseen classes. (b) Performance comparison of existing methods and ours on base and novel classes.

For example, CoCoOP [43] generates input-conditioned tokens for each instance rather than specific classes, thus making it less sensitive to class shift. (ii) Maintain consistency between the prompt model and the frozen CLIP features to achieve the original generalization ability for new tasks [15, 39]. PromptSRC [15], for instance, introduces knowledge distillation techniques to maintain consistency between the prompt model and the original CLIP features and logits. Although these methods help prevent prompt overfitting and improve model generalization to some extent, the performance improvements for unseen classes are

quite limited. As shown in Figure 1 (b), the latest SOTA method, TCP, achieves only a **0.22%** performance improvement on new classes compared to other SOTA methods (e.g., MaPLe). Therefore, this motivates us to explore the *underlying reasons* for the decline in generalization ability in B2N tasks.

We visualized the attention maps of the original CLIP model and the CoOp [44] on base and novel class in Figure 1 (a). We can observe that zero-shot generalization ability is reduced primarily due to overfitting the prompt model to base class data during the few-shot fine-tuning stage. Specifically, after fine-tuning on the base classes, the CoOp prompt model (right one) tends to focus excessively on fine-grained foreground details (e.g., concentrating attention on specific areas of the cat) while neglecting coarse-grained structural elements such as contours, shapes, and poses (e.g., the original CLIP model has a broader attention span). These structural attributes are crucial for preventing overfitting and enhancing generalization to unseen new classes. Therefore, during the prompt learning process, we aim to focus on the structural information of the image rather than fine-grained foreground details to address the B2N problem.

We propose the **Less Overfitting for Better Generalization (LOBG)** framework, as a way for learning structural information from the data, which can effectively adapt the prompt model to unseen tasks.

First, we propose the foreground information filtering (FIF) module, which removes fine-grained information from images to enable the model to focus on overall structural information rather than excessively on foreground details. Specifically, we employ the attention maps from the frozen CLIP module as masks and set appropriate thresholds to eliminate foreground details in the images. Our research shows that this moderate refinement of fine-grained information has little impact on base class training but significantly enhances the model’s generalization performance. Secondly, mainstream methods (ii) aim to restore generalization by aligning models with the original CLIP features. However, they often use strict distillation, which results in the model absorbing an excess of fine-grained information from CLIP, thereby limiting the learning capacity of the prompts and hindering improvements in generalization ability. As shown in Figure 1 (b), PromptSRC only improved performance on new classes by 0.80% compared to CLIP. In contrast, we propose the structural topology preservation (STP) constraint, which ensures consistency with the original CLIP only in terms of overall structure and our method achieves a significant improvement of 2.82% over CLIP on new classes. While preserving CLIP’s original generalization ability by maintaining its topological structure, this approach does not constrain the prompt’s adaptability to downstream tasks. Our research

indicates that focusing on extracting structural information from CLIP, rather than its details, can more effectively enhance the prompt model’s generalization ability for unseen tasks. Furthermore, we employ hierarchical logit distillation (HLD) at the output layer to complement the STP constraint, ensuring the preservation of structural information.

In summary, our method makes the following main contributions:

- We explore the decline of generalization in B2N tasks caused by overfitting to fine-grained details and propose the LOBG framework to address this problem.
- We use FIF to remove fine-grained details of images, shifting the focus to overall structure and enhancing generalization without affecting base class training.
- We introduce STP and HLD constraints, which preserve CLIP’s overall structure and generalization ability, leading to significant performance improvements on new classes compared to CLIP.
- Experiments on 11 benchmark datasets demonstrate that our method effectively mitigates overfitting of base-to-novel generalization.

## 2. Related Works

**Vision-Language Model Pre-training.** In recent years, vision-language models have garnered widespread attention from researchers as a new tool for visual recognition. Vision-language models such as CLIP [27], BLIP [18], ALIGN [12], and FILIP [40] leverage image-text pairs from the web to train multimodal networks. During pre-training, these models use a self-supervised approach by pulling closer the matched image-text pairs and pushing apart the unmatched ones. This allows the models to understand the semantics of images and their corresponding textual descriptions. Due to their strong generalization capabilities, vision-language models have been widely applied in various downstream visual tasks [1, 24, 28, 41, 45].

**Prompt Tuning.** To quickly transfer VLM to downstream tasks, some methods have adopted the concept of prompt tuning from the NLP field [14, 43, 44]. This approach introduces a small number of additional parameters to enable the rapid transfer of VLMs to downstream tasks. CoOp [44] and CoCoOp [43] fine-tune the frozen CLIP model by adding prompts to the text branch. Maple [14] and IVLP [29] enhance transferability by adding prompts to both the visual and language branches of CLIP. PromptSRC [15], KgCoOp [38] and TCP [39] attempt to improve generalization performance by incorporating knowledge distillation, introducing the knowledge of the frozen CLIP into the prompts. However, these methods still struggle to prevent CLIP from overfitting to base classes during transfer to downstream tasks, failing to meet the generalization requirements for novel classes. It is worth noting that some methods [34, 36, 42] introduced external data or ex-

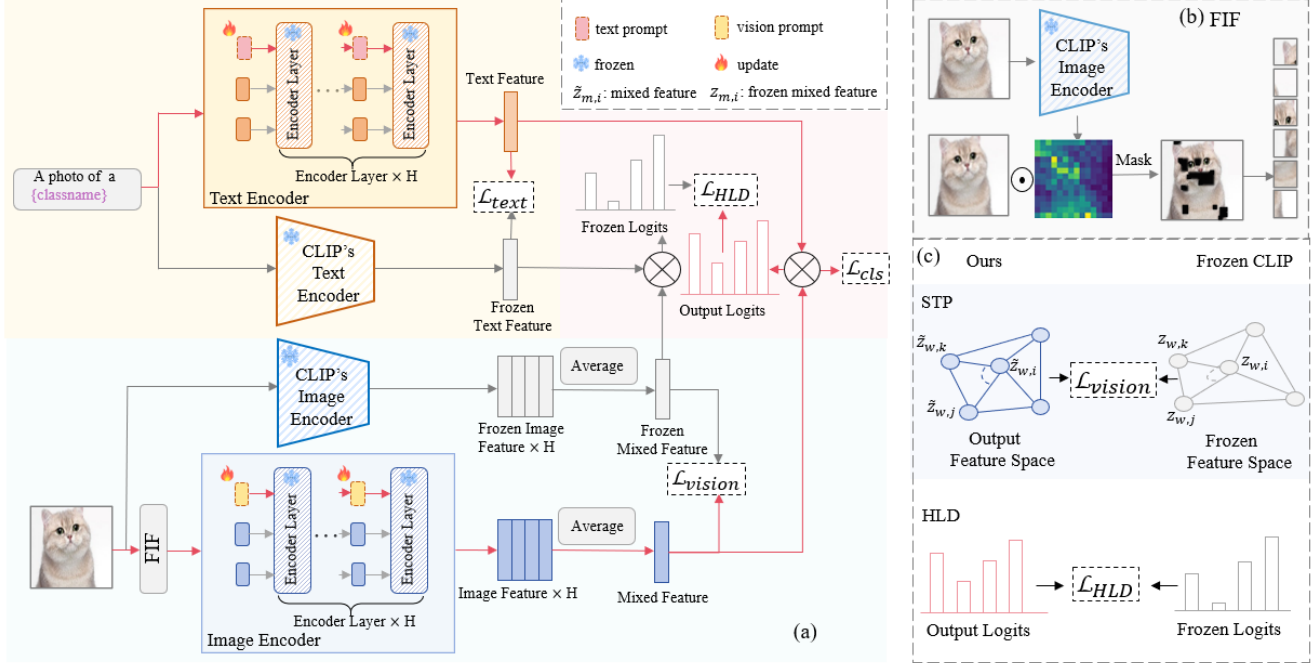


Figure 2. An overview of our method. Subfigure (a) shows the training pipeline of our method, where the text prompts and vision prompts are learnable. Subfigure (b) presents the FIF process of our method. Through FIF, the high-attention areas of the image are filtered out. Subfigure (c) presents the alignment strategy of our method. By STP and HLD, we preserve CLIP’s original generalization ability by maintaining its topological structure and does not constrain the prompt’s adaptability to downstream tasks

ternal LLMs, and some methods [19] had data leakage or used larger models. We excluded comparisons with these methods.

**Knowledge Distillation.** In deep learning, incorporating knowledge distillation has proven to enable student models to acquire knowledge from teacher models at a low cost [11, 32]. Recently, instance-level logits alignment [11, 22], multi-level logits alignment [13], and feature alignment [3, 26, 31] have become key methods for promoting knowledge transfer. In our work, however, we adopt a different distillation approach: by maintaining the original feature space of CLIP and utilizing hierarchical model information, we achieve better results for the CLIP Base-to-Novel transfer task compared to traditional single-scale knowledge distillation methods.

### 3. Method

#### 3.1. Preliminary

**Contrastive Language-Image Pretraining (CLIP).** CLIP [27] consists of two sub-networks, referred to as the image encoder and the text encoder. By understanding image-text pairs, CLIP constructs a shared embedding space  $\mathbb{R}^d$ , where  $d$  denotes the feature embedding di-

mension. The image encoder and text encoder of CLIP are denoted as  $f(\theta_f)$  and  $g(\theta_g)$ , where  $\theta_f$  and  $\theta_g$  represent the parameters of  $f$  and  $g$ . Given an image  $x$  and class labels  $\mathbf{Y} = \{y_1, y_2, \dots, y_i, \dots, y_N\}$  ( $N$  is the number of classes), the image encoder generates the corresponding image feature  $\mathbf{z} = f(x, \theta_f) \in \mathbb{R}^d$ . The text encoder then generates the corresponding text features  $\mathbf{V} = \{\mathbf{v}_i = g(\mathbf{t}_i, \theta_g) \in \mathbb{R}^d\}_{i=1}^N$  using handcrafted text templates  $\mathbf{t}_i = \text{“a photo of [CLASSNAME}_i\text{]}”$ .

Finally, using cosine similarity, CLIP predicts the class for a given image  $x$ :

$$p(\mathbf{y} = i | x) = \frac{\exp(\text{sim}(\mathbf{z}, \mathbf{v}_i) / \tau)}{\sum_{j=1}^N \exp(\text{sim}(\mathbf{z}, \mathbf{v}_j) / \tau)} \quad (1)$$

here,  $\text{sim}(\mathbf{z}, \mathbf{v}_j) = \frac{\mathbf{z} \cdot \mathbf{v}_j}{\|\mathbf{z}\| \times \|\mathbf{v}_j\|}$  denotes the cosine similarity, and  $\tau$  is the temperature coefficient.

**Soft Prompt Tuning.** Based on IVLP [29], we add learnable visual and text prompts to the image and text encoders, denoted as  $\mathbf{P}_v = \{\mathbf{p}_v^i\}_{i=1}^K$  and  $\mathbf{P}_l = \{\mathbf{p}_l^i\}_{i=1}^L$ , respectively. Here,  $K$  and  $L$  represent the number of learnable tokens. Therefore, the inputs to the image and text encoders become:  $\tilde{\mathbf{x}} = [\mathbf{P}_v, x]$  and  $\tilde{\mathbf{t}}_i = [\mathbf{P}_l, \mathbf{t}_i]$ . The resulting image feature is  $\tilde{\mathbf{z}} = f(\tilde{\mathbf{x}}, \theta_f) \in \mathbb{R}^d$ , and the text features are  $\tilde{\mathbf{V}} = \{\tilde{\mathbf{v}}_i = g(\tilde{\mathbf{t}}_i, \theta_g) \in \mathbb{R}^d\}_{i=1}^N$ . Similarly, the prediction

for a given image  $x$  in CLIP is:

$$\tilde{p}(\mathbf{y} = i|x) = \frac{\exp(\text{sim}(\tilde{z}, \tilde{\mathbf{v}}_i)/\tau)}{\sum_{j=1}^N \exp(\text{sim}(\tilde{z}, \tilde{\mathbf{v}}_j)/\tau)} \quad (2)$$

To further optimize the prompts and make them more suitable for the downstream dataset  $\mathcal{D}$ , Cross-Entropy loss is used for optimization, as follows:

$$\mathcal{L}_{cls} = -\frac{1}{N_D} \sum_{i=1}^{N_D} (\mathbf{y}_i \cdot \log(\tilde{\mathbf{p}}_i)) \quad (3)$$

here,  $N_D$  is the number of exemplars in the downstream dataset  $\mathcal{D}$ , and  $\mathbf{y}_i$  and  $\tilde{\mathbf{p}}_i$  are the true label and the predicted value for the downstream data  $x_i$ , respectively.

### 3.2. Foreground Information Filtering

VLMs are transferred to downstream tasks through prompt tuning, which enhances the model’s focus on fine-grained foreground information within the training data, facilitating effective transfer. However, in B2N tasks involving unseen downstream challenges, prompt tuning can cause the model to overly fit the training data, leading to the neglect of essential underlying visual information and ultimately degrading performance on unseen data.

To address the overfitting issue mentioned above, we propose a mask mechanism to reduce excessive attention to local information. We use the attention map of each training image to capture its foreground information and construct a mask to filter part of them. Specifically, we apply a threshold to the attention maps: attention blocks with values greater than the threshold are set to 0, while the rest are set to 1, to create a mask.

Then, we use the obtained mask to filter the foreground fine-grained information of the image:

$$\mathbf{x}' = \text{mask} \odot \mathbf{x} \quad (4)$$

where the  $\odot$  denotes element-wise multiplication. By using a mask, we can filter out the parts of the input image that are most likely to cause overfitting. This forces the model to focus more on the underlying visual information when transferring to downstream tasks. This approach helps improve the model’s ability to generalize to unknown data in downstream tasks.

### 3.3. Structural Topology Preservation

Our model aims to guide the overall feature space towards downstream tasks while preserve the original information for maintaining the generalization ability. By retaining **angular relationships between samples** instead of point-to-point constraints, we preserve the topological structure of original CLIP. This maintains CLIP’s generalization ability without limiting prompt adaptability to downstream tasks.

Given any three samples  $x_i, x_j, x_k$  in the feature topology space, they form a local angular relationship  $\mathbf{A}$ , where  $\mathbf{A}$  is used for the frozen CLIP, and  $\tilde{\mathbf{A}}$  is used for the model after prompt tuning.

Due to the different semantic information contained in various layers of ViT, we perform weighted combinations of features from different ViT layers to further supplement the lost low-level visual information during the model fitting process. The fused image feature is obtained as follows:

$$\mathbf{z}_w = \sum_{i=1}^H w_i \cdot \mathbf{z}_i \quad (5)$$

where  $\mathbf{z}_i$  is the feature from the  $i$ -th ViT layer of the image encoder,  $H$  is the number of ViT layers, and  $w_i$  is the weight obtained through Gaussian sampling, with  $\sum_i w_i = 1$ .

Therefore, for the frozen CLIP model, the local angular relationship  $\mathbf{A}$  of samples  $x_i, x_j, x_k$  is expressed as:

$$\mathbf{A}(x_i, x_j, x_k) = \frac{\mathbf{e}_{ij} \cdot \mathbf{e}_{kj}}{\|\mathbf{e}_{ij}\| \|\mathbf{e}_{kj}\|} \quad (6)$$

where  $\mathbf{e}_{ij} = \mathbf{z}_{w,i} - \mathbf{z}_{w,j}$  and  $\mathbf{e}_{kj} = \mathbf{z}_{w,k} - \mathbf{z}_{w,j}$  represent the distance vectors between two samples in the feature space.

Similarly, for the model after prompt tuning, the local angular relationship  $\tilde{\mathbf{A}}$  of samples  $x_i, x_j, x_k$  is expressed as:

$$\tilde{\mathbf{A}}(x_i, x_j, x_k) = \frac{\tilde{\mathbf{e}}_{ij} \cdot \tilde{\mathbf{e}}_{kj}}{\|\tilde{\mathbf{e}}_{ij}\| \|\tilde{\mathbf{e}}_{kj}\|} \quad (7)$$

where  $\tilde{\mathbf{e}}_{ij} = \tilde{\mathbf{z}}_{w,i} - \tilde{\mathbf{z}}_{w,j}$  and  $\tilde{\mathbf{e}}_{kj} = \tilde{\mathbf{z}}_{w,k} - \tilde{\mathbf{z}}_{w,j}$ . The local angular relationship function between samples reflects the angular structure of the feature topology space. We aim to maintain this structure during the CLIP’s transfer to downstream tasks. Therefore, our structural topology preservation loss is as follows:

$$\mathcal{L}_{vision}(x_i, x_j, x_k) = \left\| \tilde{\mathbf{A}} - \mathbf{A} \right\|_1 \quad (8)$$

Due to the sparse and relatively fixed nature of textual information, to maintain consistency in the text space, we use the L1 distance to constrain the text space for a given text  $t$ :

$$\mathcal{L}_{text} = \left\| g(\tilde{\mathbf{t}}, \theta_g) - g(\mathbf{t}, \theta_g) \right\|_1 \quad (9)$$

where the  $g(\theta_g)$  is the text encoder,  $\tilde{\mathbf{t}}$  is the text input with the prompt added, and  $\mathbf{t}$  is the original text input.

Our STP does not directly constrain the movement of individual samples in the feature space. Instead, it constrains the change in feature space structure by maintaining angular relationships, allowing reasonable displacement of samples in the feature space during the optimization process. This soft constraint is easier to optimize and imparts a degree of plasticity to the feature space, making its structure flexible.

Overall, our STP loss is defined as follows:

$$\mathcal{L}_{STP} = \mathcal{L}_{vision} + \mathcal{L}_{text} \quad (10)$$

### 3.4. Hierarchical Logit Distillation

To further complement STP at the model output and inherit CLIP’s knowledge of the relationships between different samples, we constrain the model output at different layers of the logits. We believe logits for a single example contain specific information, and distilling knowledge from them may alter the encompassing topological structure. Hence, we use hierarchical logit distillation for model consistency supplementation.

**Instance-aware Distillation.** Following the traditional knowledge distillation approach [11], we use KL divergence to achieve alignment with the frozen CLIP space at the instance awareness as follows:

$$\begin{aligned} \mathcal{L}_{ikd} &= \mathcal{D}_{KL}(\mathbf{p}(\mathbf{y}|\mathbf{x}) \parallel \tilde{\mathbf{p}}(\mathbf{y}|\mathbf{x})) \\ &= \sum_i \mathbf{p}(\mathbf{y} = i|\mathbf{x}) \log \left( \frac{\mathbf{p}(\mathbf{y} = i|\mathbf{x})}{\tilde{\mathbf{p}}(\mathbf{y} = i|\mathbf{x})} \right) \end{aligned} \quad (11)$$

here,  $\mathbf{p}$  represents the logits from the frozen CLIP, while  $\tilde{\mathbf{p}}$  represents the logits from the prompt-tuned model. The loss function  $\mathcal{L}_{ikd}$  aligns the model with the frozen CLIP at the instance awareness, providing fundamental spatial alignment.

**Class-aware Distillation.** We consider that the output of the prompt-tuned model and the output of the frozen CLIP model should exhibit similar distribution descriptions across categories.

We denote  $M$  and  $\tilde{M}$  as the class relationship matrices for the frozen CLIP and the model after prompt tuning, respectively. Given the logits  $\mathbf{p}$  of the frozen CLIP and the logits  $\tilde{\mathbf{p}}$  of prompt-tuned model, they are computed as follows:

$$M = \mathbf{p}^T \cdot \mathbf{p}, \quad \tilde{M} = \tilde{\mathbf{p}}^T \cdot \tilde{\mathbf{p}} \quad (12)$$

here,  $M$  and  $\tilde{M}$  are  $C \times C$  matrices, where  $C$  is the number of classes.  $M_{ij}$  and  $\tilde{M}_{ij}$  represent the probabilities that a sample belongs simultaneously to class  $i$  and class  $j$ .

Given the class relationship matrices, the following constraints apply:

$$\mathcal{L}_{ckd} = \frac{1}{C} \left\| M - \tilde{M} \right\|_2 \quad (13)$$

Through  $\mathcal{L}_{ckd}$ , we further supplement the lost class information during the model transfer process, achieving model consistency at the class awareness.

Our hierarchical logit distillation is:

$$\mathcal{L}_{HLD} = \mathcal{L}_{ikd} + \mathcal{L}_{ckd} \quad (14)$$

Overall, our final loss function is as follows:

$$\mathcal{L} = \mathcal{L}_{cls} + \lambda \mathcal{L}_{HLD} + \gamma \mathcal{L}_{STP} \quad (15)$$

where,  $\gamma$  and  $\lambda$  are hyperparameters.

## 4. Experiments

### 4.1. Experimental Setup

**Base-to-Novel Generalization.** In this setup, we evaluate the generalization of LOBG. Following CoOp [44], we divide the dataset evenly into two parts: base classes and novel classes. We conduct 16-shot learning on the base classes and perform zero-shot evaluation on the novel classes. This setup aims to evaluate the model’s generalization capability when transferring to downstream tasks.

**Cross-Dataset Transfer.** Following CoOp [44], in *cross-dataset transfer*, we conduct few-shot training on ImageNet1k [5] and then perform zero-shot testing on multiple heterogeneous datasets.

**Domain Generalization.** We evaluated the robustness of our method on out-of-distribution datasets. Similar to *cross-dataset* evaluation, we perform few-shot learning directly on ImageNet1K [5] and then test our ImageNet-trained model on four other ImageNet datasets that contain different types of domain shifts.

**Datasets.** For *base-to-novel generalization* and *cross dataset transfer* setting, we use ImageNet [5], FGVC Aircraft [21], EuroSAT [8], UCF101 [33], DTD [4], Caltech101 [7], Oxford-Pets [25], Stanford-Cars [16], Oxford-Flowers [23], Food101 [2], and SUN397 [37]. For *domain generalization*, we use ImageNet1k [5] as the source domain and ImageNet-A [10], ImageNet-R [9], ImageNet-V2 [30], and ImageNet-Sketch [35] as the target domains. For *base-to-novel generalization*, based on the performance of CoOp, we classify DTD [4], FGVC Aircraft [21], EuroSAT [8], and UCF101 [33] as challenging datasets. These four datasets have fine-grained characteristics, making them more prone to overfitting compared to other datasets.

**Implementation Details.** Our implementation is based on the ViT-B/16 variant of the CLIP model, utilizing prompts of length 4 in both the visual and text branches. We trained for 20 epochs across all three benchmarks. For Base-to-Novel Generalization, prompts were added in the first 7 transformer layers, while for the other two benchmarks, this number was 3. We employed the Adam optimizer with a learning rate set to 2.5e-3 and a batch size of 4. Performance metrics included base class accuracy, novel class accuracy, and harmonic mean accuracy, averaged over 3 experimental runs to determine final accuracy. We use Independent Vision-Language Prompting (IVLP) [29] as our baseline method.

### 4.2. Base-to-Novel Generalization

We compared our method with zero-shot CLIP, CoOp, Co-CoOp, Maple, PromptSRC, Dept and TCP. Table 1 shows the results across 11 datasets. Additionally, based on CoOp’s degree of overfitting and the fine-grained nature of the datasets, we classified FGVC Aircraft, EuroSAT, DTD,

(a) Average over 4 challenging datasets.

(b) Average over 7 easy datasets.

(c) Average over 11 datasets.

Method	Base	Novel	HM	Method	Base	Novel	HM	Method	Base	Novel	HM
CLIP	51.86	59.44	55.39	CLIP	79.33	82.67	80.96	CLIP	69.34	74.22	71.70
CoOp	74.19	43.57	54.90	CoOp	87.55	74.45	80.47	CoOp	82.69	63.22	71.66
CoCoOp	70.06	53.30	60.54	CoCoOp	86.42	82.20	84.26	CoCoOp	80.47	71.69	75.83
MaPLe	73.72	61.67	67.16	MaPLe	87.17	82.84	84.95	MaPLe	82.28	75.14	78.55
PromptSRC*	<u>75.88</u>	60.96	67.61	PromptSRC*	<u>88.83</u>	83.06	<u>85.84</u>	PromptSRC*	<u>84.12</u>	75.02	79.31
Dept	75.06	60.57	67.04	Dept	88.51	83.31	85.83	Dept	83.62	75.04	79.10
TCP	<u>75.88</u>	<u>62.00</u>	<u>68.24</u>	TCP	<b>88.85</b>	82.99	85.82	TCP	<b>84.13</b>	<u>75.36</u>	<u>79.51</u>
<b>Ours</b>	<b>75.97</b>	<b>65.43</b>	<b>70.29</b>	<b>Ours</b>	88.63	<b>83.67</b>	<b>86.08</b>	<b>Ours</b>	84.01	<b>77.04</b>	<b>80.37</b>

Table 1. Compare the performance on 4 challenging datasets, 7 easy datasets and all 11 datasets of our method with existing methods on base-to-novel generalization. For base-to-novel generalization, based on the performance of CoOp, we classify DTD, FGVCIAircraft, EuroSAT, and UCF101 as challenging datasets. ‘\*’ denote the performance obtained by TCP [39]. These four datasets have fine-grained characteristics, making them more prone to overfitting compared to other datasets. The best results are in **bold** and the second-best results are underlined.

	Novel											
	ImageNet	Caltech101	OxfordPets	StanfordCars	Flowers102	Food101	Aircraft	SUN397	DTD	EuroSAT	UCF101	Average
CLIP	68.14	94.00	97.26	74.89	<b>77.80</b>	91.22	36.29	75.35	59.90	64.05	77.50	74.22
CoOp	67.88	89.81	95.29	60.40	59.67	82.26	22.30	65.89	41.18	54.74	56.05	63.22
CoCoOp	70.43	93.81	97.69	73.59	71.75	91.29	23.71	76.86	56.00	60.04	73.45	71.69
MaPLe	<u>70.54</u>	94.36	<u>97.76</u>	74.00	72.46	<b>92.05</b>	35.61	<u>78.70</u>	<u>59.18</u>	73.23	78.66	75.14
PromptSRC*	<b>70.70</b>	93.90	97.40	74.73	76.77	91.50	<u>36.97</u>	<b>79.00</b>	57.50	68.43	78.33	75.02
Dept(CVPR2024)	70.13	<u>94.60</u>	97.23	<u>75.47</u>	76.37	91.60	34.83	77.80	59.13	71.07	77.23	75.04
TCP(CVPR2024)	69.87	<b>94.67</b>	97.20	74.13	75.57	91.37	34.43	78.20	58.07	<u>74.73</u>	<b>80.77</b>	<u>75.36</u>
<b>Ours</b>	70.06	94.47	<b>98.10</b>	<b>75.51</b>	<u>77.20</u>	<u>91.90</u>	<b>37.10</b>	78.47	<b>64.20</b>	<b>80.61</b>	<u>79.80</u>	<b>77.04</b>

Table 2. Compare the performance on novel classes of our method with existing methods on base-to-novel generalization. ‘\*’ denote the performance obtained by TCP [39].

	Base											
	ImageNet	Caltech101	OxfordPets	StanfordCars	Flowers102	Food101	Aircraft	SUN397	DTD	EuroSAT	UCF101	Average
CLIP	72.43	96.84	91.17	63.37	72.08	90.10	27.19	69.36	53.24	56.48	70.53	69.34
CoOp	76.47	98.00	93.67	78.12	97.60	88.33	40.44	80.60	79.44	92.19	84.69	82.69
CoCoOp	75.98	97.96	95.20	70.49	94.87	90.70	33.41	79.74	77.01	87.49	82.33	80.47
MaPLe	76.66	97.74	95.43	72.94	95.92	<u>90.71</u>	37.44	80.82	80.36	<b>94.07</b>	83.00	82.28
PromptSRC*	<u>77.60</u>	98.13	<u>95.50</u>	78.40	<u>97.90</u>	90.63	42.30	<b>82.83</b>	81.90	<u>92.40</u>	86.93	<u>84.12</u>
Dept(CVPR2024)	77.03	<u>98.30</u>	94.33	<u>79.13</u>	<b>98.00</b>	90.50	<b>43.20</b>	82.33	82.20	89.03	85.80	83.62
TCP(CVPR2024)	77.27	98.23	94.67	<b>80.80</b>	97.73	90.57	41.97	<u>82.63</u>	<b>82.77</b>	91.63	<b>87.13</b>	<b>84.13</b>
<b>Ours</b>	<b>77.91</b>	<b>98.74</b>	<b>95.60</b>	77.39	97.40	<b>90.81</b>	43.11	<u>82.63</u>	<u>82.30</u>	91.32	<u>87.00</u>	84.01

Table 3. Compare the performance on base classes of our method with existing methods on base-to-novel generalization. ‘\*’ denote the performance obtained by TCP [39].

and UCF101 as challenging datasets. Their overall accuracy is shown in Table 2. Overall, all current methods outperform CLIP on base classes, but their performance on novel classes shows limited improvement compared to CLIP and

remains stagnant.

The stagnation in novel class performance indicates that existing methods overfit to fine-grained base class details, compromising CLIP’s ability to capture fundamental visual

	Source	Target										
	ImageNet	Caltech101	OxfordPets	StanfordCars	Flowers102	Food101	Aircraft	SUN397	DTD	EuroSAT	UCF101	Average
CLIP	66.70	93.70	89.10	65.70	70.70	85.90	<b>24.90</b>	62.60	44.30	48.30	67.60	65.24
CoOp	<b>71.51</b>	93.70	89.14	64.51	68.71	85.30	18.47	64.15	41.92	46.39	66.55	63.88
CoCoOp	71.02	<b>94.43</b>	90.14	65.32	<u>71.88</u>	86.06	22.94	<u>67.36</u>	45.73	45.37	68.21	65.74
MaPLe	70.72	93.53	<u>90.49</u>	65.57	<b>72.23</b>	<u>86.20</u>	<u>24.74</u>	67.01	46.49	48.06	68.69	<u>66.30</u>
PromptSRC	<u>71.27</u>	93.60	<u>90.25</u>	<b>65.70</b>	70.25	86.15	23.90	67.10	<b>46.87</b>	45.50	<u>68.75</u>	65.81
<b>Ours</b>	71.11	<u>93.80</u>	<b>91.03</b>	65.48	71.57	<b>86.60</b>	24.11	<b>67.53</b>	<u>46.68</u>	<b>49.00</b>	<b>68.95</b>	<b>66.50</b>

Table 4. Compare the performance of our method with existing methods in cross-dataset transfer evaluation. Overall, our method demonstrates the highest generalization ability on 5 datasets, shows the second-best generalization ability on 3 datasets, and achieves the highest average accuracy.

features necessary for effective transfer. Our method better captures underlying visual information, providing greater feature space flexibility, reducing overfitting, and improving generalization.

Table 2 and Table 1 demonstrates that our method outperforms TCP on the Base-to-Novel task, with improvements of **4.47%**, and **2.68%** on novel classes, and harmonic mean across four challenging datasets. Across all eleven datasets, we achieve a third-best 84.01% on base classes, just 0.12% behind TCP, but achieve the best results of 77.04% and 80.37% on novel classes and harmonic mean, surpassing TCP by **1.68%** and **0.86%**, respectively. For further comparisons, please refer to the Appendix.

### 4.3. Cross-Dataset Transfer

Table 4 shows the results of our cross-dataset transfer experiments. On the source dataset ImageNet, our method performs comparably to other methods, only slightly behind CoOp and PromptSRC. However, compared to these two methods, our approach shows better generalization performance on 10/10 and 8/10 datasets, respectively, indicating that our method is more advantageous for cross-dataset zero-shot transfer. For detailed results, please refer to the Appendix.

### 4.4. Domain Generalization

Table 5 shows the performance of our method compared to previous methods on out-of-distribution (OOD) datasets. We conducted 16-shot training on the ImageNet dataset and then directly evaluated on the target datasets. Our method achieved the second-best accuracy on the target datasets, demonstrating that our approach can effectively transfer to datasets with domain differences even when faced with out-of-distribution scenarios.

	Source	Target				
	ImageNet	-V2	-S	-A	-R	Avg.
CLIP	66.73	60.83	46.15	47.77	73.96	57.18
CoOp	71.51	64.20	47.99	49.71	75.21	59.28
CoCoOp	71.02	64.07	48.75	50.63	76.18	59.91
MaPLe	70.72	64.07	49.15	50.90	76.98	60.27
PromptSRC	<u>71.27</u>	64.35	<b>49.55</b>	50.90	<b>77.80</b>	<b>60.65</b>
TCP	71.20	<b>64.60</b>	49.50	<b>51.20</b>	76.73	60.51
<b>Ours</b>	71.11	64.47	49.30	50.91	<u>77.76</u>	<u>60.61</u>

Table 5. Domain generalization. Prompt learning methods are trained on ImageNet and evaluated on datasets with domain shifts.

### 4.5. Ablation Studies

Methods	STP	HLD	FIF	Acc(%)		
				Base	Novel	HM
baseline				73.77	54.63	62.77
+STP	✓			74.85	61.93	67.78
+HLD		✓		74.95	59.93	66.60
+FIF			✓	72.03	60.43	65.73
+STP+HLD	✓	✓		<b>76.54</b>	63.83	69.61
+STP+HLD+FIF	✓	✓	✓	75.93	<b>65.43</b>	<b>70.29</b>

Table 6. Effectiveness of our proposed techniques. Results are averaged over 4 challenging datasets. HM stands for harmonic mean.

**Effectiveness of different components.** We conducted ablation experiments by gradually removing Foreground Information Filtering (FIF), STP and HLD to evaluate their contributions to preventing model overfitting and alleviating the B2N problem. Table 6 shows the contributions of each component.

We observed that baseline performs well on base classes but poorly on novel classes. Applying STP improves novel class performance by 7.3%. Using HLD, the model maintains novel class gains while enhancing base class performance. This shows that preserving topological structure and output consistency with the frozen CLIP helps retain model plasticity, promoting task transfer and generalization.

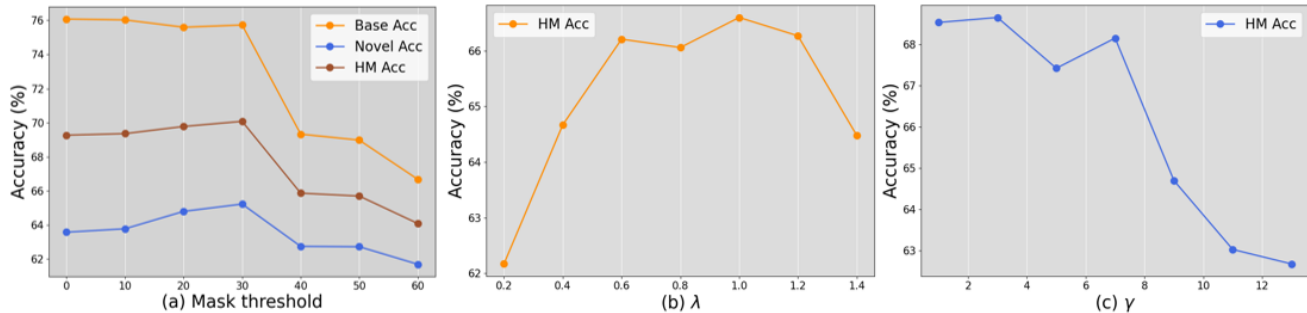


Figure 3. The effect of mask thresholds and sensitivity analysis of  $\gamma$  and  $\lambda$ .

Finally, incorporating FIF further enhances generalization, increasing novel class performance by 1.60% with minimal impact on base classes, confirming our view on overfitting in B2N tasks. More detailed ablation results are provided in the Appendix.

Method	Base Acc.	Novel Acc.	HM
baseline	73.77	54.63	62.77
1: + $\mathcal{L}_1$	73.96	60.05	66.28
2: + $\mathcal{L}_2$	74.50	58.57	65.58
3: +STP (Ours)	74.85	61.93	67.78

Table 7. Effectiveness of structural topology preservation on 4 challenging datasets. Our structural topology preservation provides better performance.

Method	Base Acc.	Novel Acc.	HM
baseline	73.77	54.63	62.77
1: + $\mathcal{D}_{KL}$	74.43	57.25	65.09
2: +HLD (Ours)	74.95	59.93	66.60

Table 8. Effectiveness of hierarchical logit distillation on 4 challenging datasets. Our hierarchical logit distillation provides better performance.

**Analysis of feature space distillation methods.** In Table 7, we discuss the performance of different feature space distillation methods. By comparing various constraint strategies, we found that our STP outperforms distance-based matching constraints in terms of generalization. This indicates that our method endows the feature space with greater plasticity, effectively avoiding overfitting and achieving better downstream task transfer. Overall, STP achieves the highest harmonic mean accuracy.

**Effectiveness of foreground information filtering.** Figure 3(a) shows the impact of reducing Foreground Information Filtering on the model. We found that removing a small portion of this information has little to no effect on the model’s learning of base classes and promotes generalization to unseen novel classes.

**Analysis of logits distillation methods.** In Table 8, we discuss the performance of different logits constraint methods. By applying hierarchical logit distillation, our method achieves better performance on both base and novel classes compared to the original KL divergence.

**Hyperparameter sensitivity analysis:**

- **Mask Threshold.** Figure 3(a) shows the impact of the Mask threshold on the harmonic mean accuracy. Overall, performance initially increases with a higher Mask threshold, but then decreases as the threshold continues to rise. Using a Mask threshold of 30 provides the highest overall harmonic mean accuracy.
- **Distillation Parameters.** Figure 3(b) and 3(c) show the impact of  $\lambda$  and  $\gamma$  on the harmonic mean accuracy. Based on the overall model performance, we choose  $\lambda = 1$  and  $\gamma = 3$  as the hyperparameters for  $\mathcal{L}_{HLD}$  and  $\mathcal{L}_{STP}$ .

**5. Conclusion and Limitation**

In this work, we introduce the LOBG framework to tackle overfitting in Base-to-Novel task, improving generalization in VLM transfer. By filtering fine-grained foreground information, we reduce overfitting and enhance attention to underlying visual details. We also develop structural topology preservation (STP) loss and hierarchical logit distillation (HLD) to preserve CLIP’s structural information while adapting to downstream tasks. Our method shows significant improvements across 11 datasets and outperforms existing approaches. Future work will focus on refining foreground filtering to minimize its impact on base class learning and developing more effective methods for capturing structural information to further address overfitting in VLM prompt tuning.

**References**

[1] Hanoona Bangalath, Muhammad Maaz, Muhammad Uzair Khattak, Salman H Khan, and Fahad Shahbaz Khan. Bridging the gap between object and image-level representations for open-vocabulary detection. *Advances in Neural Information Processing Systems*, 35:33781–33794, 2022. 2



- [2] Lukas Bossard, Matthieu Guillaumin, and Luc Van Gool. Food-101—mining discriminative components with random forests. In *Computer Vision—ECCV 2014: 13th European Conference, Zurich, Switzerland, September 6–12, 2014, Proceedings, Part VI 13*, pages 446–461. Springer, 2014. 5
- [3] Defang Chen, Jian-Ping Mei, Yuan Zhang, Can Wang, Zhe Wang, Yan Feng, and Chun Chen. Cross-layer distillation with semantic calibration. In *Proceedings of the AAAI conference on artificial intelligence*, pages 7028–7036, 2021. 3
- [4] Mircea Cimpoi, Subhansu Maji, Iasonas Kokkinos, Sammy Mohamed, and Andrea Vedaldi. Describing textures in the wild. In *Proceedings of the IEEE conference on computer vision and pattern recognition*, pages 3606–3613, 2014. 5
- [5] Jia Deng, Wei Dong, Richard Socher, Li-Jia Li, Kai Li, and Li Fei-Fei. Imagenet: A large-scale hierarchical image database. In *2009 IEEE conference on computer vision and pattern recognition*, pages 248–255. Ieee, 2009. 5
- [6] Jian Ding, Nan Xue, Gui-Song Xia, and Dengxin Dai. Decoupling zero-shot semantic segmentation. In *Proceedings of the IEEE/CVF Conference on Computer Vision and Pattern Recognition*, pages 11583–11592, 2022. 1
- [7] Li Fei-Fei, Rob Fergus, and Pietro Perona. Learning generative visual models from few training examples: An incremental bayesian approach tested on 101 object categories. In *2004 conference on computer vision and pattern recognition workshop*, pages 178–178. IEEE, 2004. 5
- [8] Patrick Helber, Benjamin Bischke, Andreas Dengel, and Damian Borth. Eurosat: A novel dataset and deep learning benchmark for land use and land cover classification. *IEEE Journal of Selected Topics in Applied Earth Observations and Remote Sensing*, 12(7):2217–2226, 2019. 5
- [9] Dan Hendrycks, Steven Basart, Norman Mu, Saurav Kadavath, Frank Wang, Evan Dorundo, Rahul Desai, Tyler Zhu, Samyak Parajuli, Mike Guo, et al. The many faces of robustness: A critical analysis of out-of-distribution generalization. In *Proceedings of the IEEE/CVF international conference on computer vision*, pages 8340–8349, 2021. 5
- [10] Dan Hendrycks, Kevin Zhao, Steven Basart, Jacob Steinhardt, and Dawn Song. Natural adversarial examples. In *Proceedings of the IEEE/CVF conference on computer vision and pattern recognition*, pages 15262–15271, 2021. 5
- [11] Geoffrey Hinton, Oriol Vinyals, and Jeff Dean. Distilling the knowledge in a neural network. *arXiv preprint arXiv:1503.02531*, 2015. 3, 5
- [12] Chao Jia, Yinfei Yang, Ye Xia, Yi-Ting Chen, Zarana Parekh, Hieu Pham, Quoc Le, Yun-Hsuan Sung, Zhen Li, and Tom Duerig. Scaling up visual and vision-language representation learning with noisy text supervision. In *International conference on machine learning*, pages 4904–4916. PMLR, 2021. 1, 2
- [13] Ying Jin, Jiaqi Wang, and Dahua Lin. Multi-level logit distillation. In *Proceedings of the IEEE/CVF Conference on Computer Vision and Pattern Recognition*, pages 24276–24285, 2023. 3
- [14] Muhammad Uzair Khattak, Hanoona Rasheed, Muhammad Maaz, Salman Khan, and Fahad Shahbaz Khan. Maple: Multi-modal prompt learning. In *Proceedings of the IEEE/CVF Conference on Computer Vision and Pattern Recognition*, pages 19113–19122, 2023. 1, 2
- [15] Muhammad Uzair Khattak, Syed Talal Wasim, Muzammal Naseer, Salman Khan, Ming-Hsuan Yang, and Fahad Shahbaz Khan. Self-regulating prompts: Foundational model adaptation without forgetting. In *Proceedings of the IEEE/CVF International Conference on Computer Vision*, pages 15190–15200, 2023. 1, 2
- [16] Jonathan Krause, Michael Stark, Jia Deng, and Li Fei-Fei. 3d object representations for fine-grained categorization. In *Proceedings of the IEEE international conference on computer vision workshops*, pages 554–561, 2013. 5
- [17] Boyi Li, Kilian Q Weinberger, Serge Belongie, Vladlen Koltun, and René Ranftl. Language-driven semantic segmentation. *arXiv preprint arXiv:2201.03546*, 2022. 1
- [18] Junnan Li, Dongxu Li, Caiming Xiong, and Steven Hoi. Blip: Bootstrapping language-image pre-training for unified vision-language understanding and generation. In *International conference on machine learning*, pages 12888–12900. PMLR, 2022. 2
- [19] Zheng Li, Xiang Li, Xinyi Fu, Xin Zhang, Weiqiang Wang, Shuo Chen, and Jian Yang. Promptkd: Unsupervised prompt distillation for vision-language models. In *Proceedings of the IEEE/CVF Conference on Computer Vision and Pattern Recognition*, pages 26617–26626, 2024. 3
- [20] Muhammad Maaz, Hanoona Rasheed, Salman Khan, Fahad Shahbaz Khan, Rao Muhammad Anwer, and Ming-Hsuan Yang. Class-agnostic object detection with multi-modal transformer. In *European conference on computer vision*, pages 512–531. Springer, 2022. 1
- [21] Subhansu Maji, Esa Rahtu, Juho Kannala, Matthew Blaschko, and Andrea Vedaldi. Fine-grained visual classification of aircraft. *arXiv preprint arXiv:1306.5151*, 2013. 5
- [22] Seyed Iman Mirzadeh, Mehrdad Farajtabar, Ang Li, Nir Levine, Akihiro Matsukawa, and Hassan Ghasemzadeh. Improved knowledge distillation via teacher assistant. In *Proceedings of the AAAI conference on artificial intelligence*, pages 5191–5198, 2020. 3
- [23] Maria-Elena Nilsback and Andrew Zisserman. Automated flower classification over a large number of classes. In *2008 Sixth Indian conference on computer vision, graphics & image processing*, pages 722–729. IEEE, 2008. 5
- [24] Maria-Elena Nilsback and Andrew Zisserman. Automated flower classification over a large number of classes. In *2008 Sixth Indian conference on computer vision, graphics & image processing*, pages 722–729. IEEE, 2008. 2
- [25] Omkar M Parkhi, Andrea Vedaldi, Andrew Zisserman, and CV Jawahar. Cats and dogs. In *2012 IEEE conference on computer vision and pattern recognition*, pages 3498–3505. IEEE, 2012. 5
- [26] Nikolaos Passalis and Anastasios Tefas. Learning deep representations with probabilistic knowledge transfer. In *Proceedings of the European Conference on Computer Vision (ECCV)*, pages 268–284, 2018. 3
- [27] Alec Radford, Jong Wook Kim, Chris Hallacy, Aditya Ramesh, Gabriel Goh, Sandhini Agarwal, Girish Sastry,

- Amanda Askell, Pamela Mishkin, Jack Clark, et al. Learning transferable visual models from natural language supervision. In *International conference on machine learning*, pages 8748–8763. PMLR, 2021. 1, 2, 3
- [28] Yongming Rao, Wenliang Zhao, Guangyi Chen, Yansong Tang, Zheng Zhu, Guan Huang, Jie Zhou, and Jiwen Lu. Denseclip: Language-guided dense prediction with context-aware prompting. In *Proceedings of the IEEE/CVF conference on computer vision and pattern recognition*, pages 18082–18091, 2022. 2
- [29] Hanoona Rasheed, Muhammad Uzair Khattak, Muhammad Maaz, Salman Khan, and Fahad Shahbaz Khan. Fine-tuned clip models are efficient video learners. In *Proceedings of the IEEE/CVF Conference on Computer Vision and Pattern Recognition*, pages 6545–6554, 2023. 2, 3, 5
- [30] Benjamin Recht, Rebecca Roelofs, Ludwig Schmidt, and Vaishaal Shankar. Do imagenet classifiers generalize to imagenet? In *International conference on machine learning*, pages 5389–5400. PMLR, 2019. 5
- [31] Adriana Romero, Nicolas Ballas, Samira Ebrahimi Kahou, Antoine Chassang, Carlo Gatta, and Yoshua Bengio. Fitnets: Hints for thin deep nets. *arXiv preprint arXiv:1412.6550*, 2014. 3
- [32] Kaiyou Song, Jin Xie, Shan Zhang, and Zimeng Luo. Multi-mode online knowledge distillation for self-supervised visual representation learning. In *Proceedings of the IEEE/CVF Conference on Computer Vision and Pattern Recognition*, pages 11848–11857, 2023. 3
- [33] Khurram Soomro, Amir Roshan Zamir, and Mubarak Shah. A dataset of 101 human action classes from videos in the wild. *Center for Research in Computer Vision*, 2(11):1–7, 2012. 5
- [34] Xinyu Tian, Shu Zou, Zhaoyuan Yang, and Jing Zhang. Argue: Attribute-guided prompt tuning for vision-language models. In *Proceedings of the IEEE/CVF Conference on Computer Vision and Pattern Recognition*, pages 28578–28587, 2024. 2
- [35] Haohan Wang, Songwei Ge, Zachary Lipton, and Eric P Xing. Learning robust global representations by penalizing local predictive power. *Advances in Neural Information Processing Systems*, 32, 2019. 5
- [36] Yubin Wang, Xinyang Jiang, De Cheng, Dongsheng Li, and Cairong Zhao. Learning hierarchical prompt with structured linguistic knowledge for vision-language models. In *Proceedings of the AAAI Conference on Artificial Intelligence*, pages 5749–5757, 2024. 2
- [37] Jianxiong Xiao, James Hays, Krista A Ehinger, Aude Oliva, and Antonio Torralba. Sun database: Large-scale scene recognition from abbey to zoo. In *2010 IEEE computer society conference on computer vision and pattern recognition*, pages 3485–3492. IEEE, 2010. 5
- [38] Hantao Yao, Rui Zhang, and Changsheng Xu. Visual-language prompt tuning with knowledge-guided context optimization. In *Proceedings of the IEEE/CVF conference on computer vision and pattern recognition*, pages 6757–6767, 2023. 2
- [39] Hantao Yao, Rui Zhang, and Changsheng Xu. Tcp: Textual-based class-aware prompt tuning for visual-language model. In *Proceedings of the IEEE/CVF Conference on Computer Vision and Pattern Recognition*, pages 23438–23448, 2024. 1, 2, 6
- [40] Lewei Yao, Runhui Huang, Lu Hou, Guansong Lu, Minzhe Niu, Hang Xu, Xiaodan Liang, Zhenguo Li, Xin Jiang, and Chunjing Xu. Filip: Fine-grained interactive language-image pre-training. *arXiv preprint arXiv:2111.07783*, 2021. 2
- [41] Yuhang Zang, Wei Li, Kaiyang Zhou, Chen Huang, and Chen Change Loy. Open-vocabulary detr with conditional matching. In *European Conference on Computer Vision*, pages 106–122. Springer, 2022. 2
- [42] Yi Zhang, Ce Zhang, Ke Yu, Yushun Tang, and Zhihai He. Concept-guided prompt learning for generalization in vision-language models. In *Proceedings of the AAAI Conference on Artificial Intelligence*, pages 7377–7386, 2024. 2
- [43] Kaiyang Zhou, Jingkang Yang, Chen Change Loy, and Ziwei Liu. Conditional prompt learning for vision-language models. In *Proceedings of the IEEE/CVF conference on computer vision and pattern recognition*, pages 16816–16825, 2022. 1, 2
- [44] Kaiyang Zhou, Jingkang Yang, Chen Change Loy, and Ziwei Liu. Learning to prompt for vision-language models. *International Journal of Computer Vision*, 130(9):2337–2348, 2022. 1, 2, 5
- [45] Xingyi Zhou, Rohit Girdhar, Armand Joulin, Philipp Krähenbühl, and Ishan Misra. Detecting twenty-thousand classes using image-level supervision. In *European Conference on Computer Vision*, pages 350–368. Springer, 2022. 2